ELSEVIER

1 March 1996

Chemical Physics Letters 250 (1996) 279–286

CHEMICAL PHYSICS LETTERS

Femtosecond elementary dynamics of transition states and asymmetric α-cleavage in Norrish reactions

Sang Kyu Kim, Ahmed H. Zewail

Arthur Amos Noyes Chemical Physics Laboratory, California Institute of Technology, Pasadena, CA 91125, USA

Received 21 December 1995

Abstract

In this Letter, we report studies of the femtosecond dynamics of transition states and asymmetric α-cleavage in Norrish type-I reactions. Systematically, we consider the dynamics of dissociation along two reaction coordinates in methyl ethyl ketone and diethyl ketone, and compare these results with those of dimethyl ketone and methyl chloro ketone. The concept of concertedness as the system moves away from the transition-state region is examined and the primary and secondary processes involved in the α-cleavage are resolved. We compare experimental results with theoretical predictions of impulsive and statistical models.

1. Introduction

Norrish type-I reactions [1] of ketones have been one of the most extensively investigated areas in photochemistry [2]. Such reactions have provided good model systems to address some important issues in photochemistry such as the dissociation mechanism [3–5], coupling of electronic states [6–8], nascent product-state distributions [9–13], and concertedness of reactions with multi-bond breaking events [9–16]. They have also been used as a convenient source of hydrocarbon free radicals, widely used in organic syntheses, and are important combustion species themselves [2].

The acetone molecule, because of its relative simplicity, has been of particular interest in numerous photochemical studies and for the investigation of dissociation at many different energies [2]. At relatively low energies ($\lambda \geqslant 266$ nm), the major dissociation channel is the cleavage of one C–C bond which is in the α-position to the carbonyl group, producing CH_3CO and CH_3 radicals. The CH_3CO radical formed does not have enough internal energy to surmount the barrier to further dissociation [17].

However, at high energies ($\lambda \leqslant 193$ nm), where Rydberg states are excited, both C–C bonds adjacent to the carbonyl group of acetone dissociate, giving two CH_3 radicals and CO as final products with a quantum yield of nearly unity [18]. This breakage of the two chemically equivalent bonds in the reaction of $(CH_3)_2CO \rightarrow 2CH_3 + CO$ has been intensively studied as a model system for resolving a fundamental issue [19,20], namely, do the two bond-breaking events occur in a *concerted* or in a *stepwise* manner?

The distinguishing criterion between the concerted and stepwise mechanisms has in the past been defined by using the internal molecular clock, the calculated rotational period ($\approx$ ps) of the intermediate [8–13]. From product-state distribution and alignment data the lifetime of the intermediate has been deduced to be longer (or shorter) than the rotational

PII S0009-2614(96)00018-8

period, inferring the mechanism of the reaction to be stepwise (or concerted). This definition of concertedness is not fundamental [15], and the direct measurement of the intermediate lifetime with femtosecond (fs) resolution is a key to the resolution of the issue of concertedness and synchronicity.

Fs-resolved mass spectrometry is a powerful approach for determining reaction pathways by probing the nuclear dynamics of the parent and/or of intermediates during the reaction [15,21,22]. For acetone [15], real-time dynamics of the dissociation, when excited to the (n–4s) Rydberg state, show two elementary steps for the two C–C bonds with distinctly different time scales for the *primary* and *secondary* α-bond breakage,

$$(CH_3)_2CO^* \rightarrow CH_3CO^{\cdot\dagger} + {}^{\cdot}CH_3 \quad (50\,\text{fs}), \qquad (1)$$

$$CH_3CO^{\cdot\dagger} \rightarrow {}^{\cdot}CH_3 + CO \quad (0.5\,\text{ps}). \qquad (2)$$

The experimental results indicate that the concertedness of the reaction should be judged from the dynamical time scale for the actual nuclear motions of the intermediate or transition states along the reaction coordinate [15]. As Eqs. (1) and (2) indicate, the two elementary steps differ in their time scales by an order of magnitude and yet both are faster than the rotational period. Therefore, the reaction mechanism would have been assigned as concerted, which is clearly not the case.

For asymmetric α-cleavage, the problem is different because the strengths of the two C–C bonds are not identical, the vibrational phase space is distinct and there are multiple reaction coordinates. With fs time resolution, the evolution of the cleavage could be followed and, with mass resolution, the transient intermediates formed along different pathways can be positively identified. Of particular interest here are the asymmetric ketones, R_1COR_2, where R_1 and R_2 are CH_3 and C_2H_5, and now the C–C bonds are of a different nature. As shown in Fig. 1, this picture has roots in transition-state spectroscopy [23] where, in this case, the preparation is into a quasi-bound state and the clocking involves two channels [8].

In this Letter, we report on the fs dynamics of the methyl ethyl ketone ($CH_3COC_2H_5$) and diethyl ketone ($C_2H_5COC_2H_5$), and compare these results with those of dimethyl ketone (CH_3COCH_3, acetone) and methyl chloro ketone (CH_3COCl), acetyl chloride. The energetics involved in the α-bond cleavage of methyl ethyl ketone and diethyl ketone are similar to those of acetone [12]. Therefore, we have an opportunity to investigate the dynamics of the *primary* and *secondary* C–C bond dissociation and to examine how they are affected as the number of internal degrees of freedom increases with the substitution of the methyl or ethyl group. We can also examine the forces influencing the primary cleavage and the extent of energy randomization in the secondary cleavage. We consider theoretical models, for qualitative and quantitative comparisons with the experimental observation, in two regimes of complete statistical behavior and a selective impulsive force.

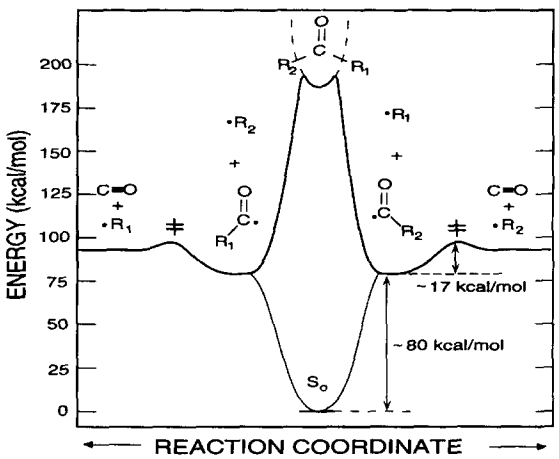

Fig. 1. Potential energy surfaces involved in the Norrish type-I reactions along the reaction coordinates (C–C bonds) leading to two different channels in the asymmetric α-cleavage of ketones: R_1COR_2, where R_1 or $R_2 = CH_3$ or C_2H_5. The approximate energetics involved in the primary and secondary C–C bond cleavage are depicted.

2. Experimental

The experimental apparatus has been described in detail elsewhere [21]. Briefly, a colliding pulse mode-locked (CPM) ring dye laser pumped by an Ar^+ laser (Coherent; 514.5 nm, 2.8–3.5 W) generated the femtosecond laser pulses (fwhm ≈ 60 fs, $\lambda \approx 615$ nm, ≈ 83 MHz). These pulses were amplified using a four-stage dye amplifier pumped by the

532 nm output of a Nd:YAG laser (Spectra-Physics, DCR-3, 20 Hz). The amplified output pulses were temporally recompressed to 60 fs in a sequence of four high-refractive-index glass prisms. The final laser output was split into two portions. One part, for the excitation of the molecule (pump), was frequency doubled using a 0.5 mm KD*P crystal to give 307 nm. The other part, for the ionization of the mass species (probe), was passed through a retroreflector on a computer-controlled actuator. The pump and probe laser pulses were recombined collinearly at a dichroic mirror and focused into the molecular beam chamber.

The molecular beam chamber consists of a two-stage pumping system divided by a ≈ 2 mm diameter skimmer. The He carrier gas was passed through the sample, methyl ethyl ketone (Sigma, 99.5%) or diethyl ketone (Aldrich, 99 + %), at room temperature with a typical backing pressure of 20 psi. The background pressure in the TOF chamber was maintained at 1×10^{-6} Torr when the nozzle (0.3 mm diameter) was open. The TOF mass spectra (with mass resolution, $m/\Delta m$, of ≈ 150) were taken using a digital oscilloscope (LeCroy 9361). The ion signal for a specific mass was selected by using a gated boxcar integrator (SR250) and monitored as a function of the delay time between the pump and probe laser pulses.

Molecules prepared in the pulsed, skimmed molecular beam were excited by a fs laser pulse to initiate the reaction. After a certain delay time, another fs laser pulse ionized the existing mass species during or after the fragmentation. The ions created were separated in the time-of-flight (TOF) mass spectrometer according to their mass-to-charge ratios. The ions were detected using microchannel plates (MCP) and the signal was processed and handled with the help of a computer.

3. Results

The TOF mass spectra taken 50 fs after time-zero for methyl ethyl ketone and diethyl ketone are shown in Fig. 2. For methyl ethyl ketone, ion signals due to the parent ($CH_3COC_2H_5$: 72 amu) and reaction intermediates, corresponding to the acetyl (CH_3CO: 43 amu) and propionyl (C_2H_5CO: 57 amu) radicals,

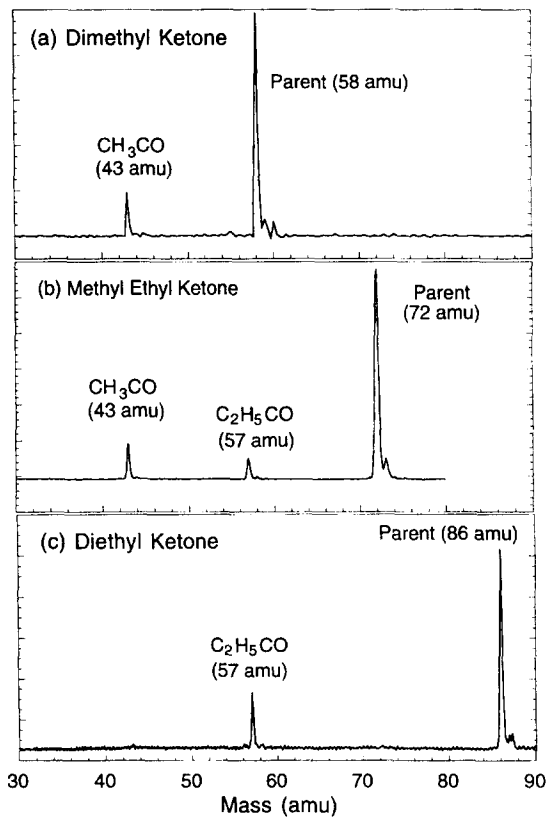

Fig. 2. TOF mass spectra of (a) dimethyl ketone, (b) methyl ethyl ketone, and (c) diethyl ketone, taken at $t \approx 50$ fs. Two different intermediates, CH_3CO and C_2H_5CO radicals, from methyl ethyl ketone are well separated in the TOF mass spectrum.

are clearly identified in the TOF mass spectrum, Fig. 2. Similarly, for diethyl ketone, ion signals due to the parent ($C_2H_5COC_2H_5$: 86 amu) and intermediate (C_2H_5CO: 57 amu) are also well separated, Fig. 2. For comparison we show the mass spectrum for acetone. The power dependence for acetone was examined [15]. For the molecules studied here the power was attenuated to the appropriate level of no signal when either the pump or the probe pulse alone intersected the molecular beam.

For both methyl ethyl ketone and diethyl ketone, the parent signal is strong at time-zero and completely disappears within a few hundred fs of the reaction time. The parent transients were fitted using a single exponential decay function with a convolution of the laser pulses [21] with a typical cross-correlation width (hwhm) of 90 ± 30 fs, Figs. 3 and 4.

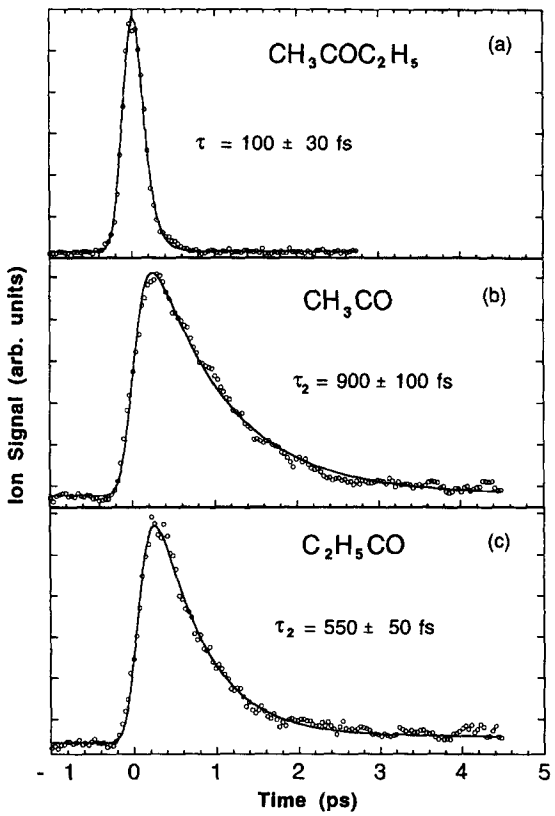

Fig. 3. Transients of (a) the parent, methyl ethyl ketone ($CH_3COC_2H_5$), (b) the acetyl radical (CH_3CO), and (c) the propionyl radical (C_2H_5CO). Theoretical fits are shown as solid lines; see text.

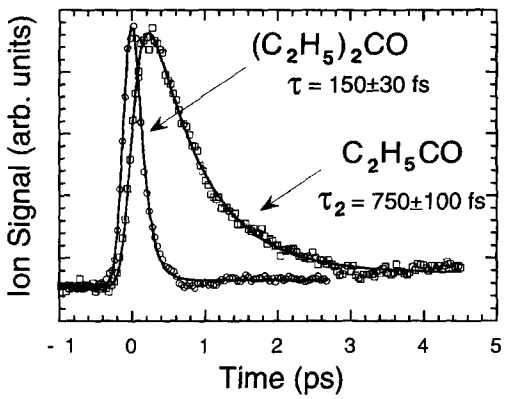

Fig. 4. Transients of diethyl ketone ($C_2H_5COC_2H_5$) and the propionyl radical (C_2H_5CO). Theoretical fits are shown as solid lines.

In contrast, the intermediate signal shows a rise-and-decay time evolution, i.e. it increases in the first few hundred fs and then decreases with further increase in the reaction time. The intermediate transients were fitted using a biexponential function as a molecular response function, $M(t) = A[\exp(-t/\tau_2) - \exp(-t/\tau_1)]$, to give τ_1 and τ_2 as the rise and decay time constants, respectively (see Figs. 3 and 4).

For methyl ethyl ketone, the parent ($CH_3COC_2H_5$) signal decays with a time constant (τ) of 100 ± 30 fs. The signals due to CH_3CO and

Table 1
Secondary cleavage: Experimental values (τ_2)and theoretical predictions of the internal energies

Parent	Intermediate	Exp. τ_2 (fs) [a]	Internal energy of intermediate [b]		
			RRKM [c]	(primary α-cleavage)	
				impulsive	statistical
acetone [d]	CH_3CO	500	35	38	53
methyl ethyl ketone	CH_3CO	900	31	38	39
acetyl chloride [e]	CH_3CO	< 100	> 55	56	82
methyl ethyl ketone	C_2H_5CO	550		42	67
diethyl ketone	C_2H_5CO	750		42	53

[a] For uncertainties of the time constants, see the text.
[b] The internal energies (kcal/mol) of the intermediates are calculated from the total available energy for the fragments from the primary bond cleavage (the photon energy minus bond dissociation energy); 186 − 80 = 106 kcal/mol for acetone [15], methyl ethyl and diethyl ketones, 186 − 83 = 103 kcal/mol for acetyl chloride [30].
[c] The internal energies estimated from the time constants (τ_2) using the RRKM calculation (see the text).
[d] Taken from Ref. [15]. [e] See Ref. [24].

C_2H_5CO radicals both rise with $\tau_1 \approx 100$ fs, which is the same as the decay time constant of the parent. However, these two intermediates decay with different time constants; the $CH_3CO^{\cdot}$ signal decays with $\tau_2 = 900 \pm 100$ fs, while the $C_2H_5CO^{\cdot}$ signal decays with $\tau_2 = 550 \pm 50$ fs, Fig. 3.

For diethyl ketone, the parent ($C_2H_5COC_2H_5$) signal decays with $\tau = 150 \pm 30$ fs, which is longer than the decay time of methyl ethyl ketone. The C_2H_5CO intermediate grows with $\tau_1 \approx 150$ fs, and decays with $\tau_2 = 750 \pm 100$ fs, Fig. 4. Time constants for the secondary C–C bond cleavage of methyl ethyl ketone and diethyl ketone are listed in Table 1 with those of acetone [15] and acetyl chloride [24].

4. Discussion

From the above results it is clear that two different α-bonds of methyl ethyl ketone are involved in a *stepwise* breakage to produce either $CH_3CO^{\cdot}$ or $C_2H_5CO^{\cdot}$ as transient intermediates. As shown in the TOF mass spectrum and the transients in Figs. 2 and 3, the parent has two channels for dissociation,

$$CH_3COC_2H_5^{*} \rightarrow CH_3CO^{\cdot\dagger} + {}^{\cdot}C_2H_5, \quad (3)$$

$$CH_3COC_2H_5^{*} \rightarrow C_2H_5CO^{\cdot\dagger} + {}^{\cdot}CH_3. \quad (4)$$

The nascent intermediates, CH_3CO or C_2H_5CO radicals, are vibrationally hot, and dissociate further through the secondary α-bond cleavage,

$$CH_3CO^{\cdot\dagger} \rightarrow {}^{\cdot}CH_3 + CO, \quad (5)$$

$$C_2H_5CO^{\cdot\dagger} \rightarrow {}^{\cdot}C_2H_5 + CO. \quad (6)$$

The dissociation of diethyl ketone, which has two equivalent C–C bonds in the α-position to the carbonyl group, is similar to that of acetone [15]; the two α-bonds break in a stepwise manner producing the C_2H_5CO radical as a reaction intermediate, which further dissociates to produce ethyl radical and CO. For both methyl ethyl ketone and diethyl ketone, no intermediates due to β-cleavage, such as CH_3COCH_2 or $C_2H_5COCH_2$ radicals, were found in our fs-resolved TOF mass spectra (see Fig. 2), indicating that the major channels for the dissociation of these ketones are the α-bond cleavages shown in Eqs. (3)–(6).

4.1. Energetics and the potential energy surface

The excitation of methyl ethyl ketone and diethyl ketone by two 307 nm photons prepares the molecule in a Rydberg state, as in the case of acetone [15]. Energies of the Rydberg series are very similar to those of acyclic ketones. At the photon energy used, the molecule is excited to the n–4s state [5,6,14], which is strongly coupled to a valence state that is dissociative in nature [5,14]. As depicted in Fig. 1, the valence state leads to an ultrafast α-bond cleavage [15], and is dissociative upon the elongation of the C–C bond in the α-position. The symmetry correlation for the molecular orbitals suggests the $n\text{–}\sigma^*(C\text{–}C)$ state, with σ^* repulsion in the C–C, correlates to the ground electronic states of the products diabatically [2,3].

The bond dissociation energies for the two different α-bonds in methyl ethyl ketone are almost equal (≈ 80 kcal/mol) [12]. Therefore, the energetics involved in the primary α-bond cleavage is similar for acetone, methyl ethyl ketone, and diethyl ketone. The secondary C–C bond cleavage, the cleavage in the CH_3CO radical, has a reaction barrier of ≈ 17 kcal/mol [11,25]. Since the electronic structure is similar for both CH_3CO and C_2H_5CO radicals, it is not unreasonable to assume the same barrier of ≈ 17 kcal/mol for the secondary C–C bond dissociation of the C_2H_5CO radical [11,12,25]. The potential energy surface depicted in Fig. 1 illustrates the adiabatic dissociation on the ground state and the diabatic correlation from the transition-state region to final products.

4.2. The primary C–C bond cleavage

The measured time constant for the primary α-bond cleavage (τ) ranges from 50–150 fs in the three molecules studied. This ultrashort time dynamics reflects a direct repulsion in the α-cleavage, without the involvement of the entire vibrational phase space. Noticeably, however, τ increases as the number of atoms in the molecule increases. For acetone, $\tau = 50$ fs, which is comparable to the vibrational period along the reaction coordinate (≈ 43 fs) [14,26]. However, as the number of internal degrees of freedom increases, the dissociation becomes

slower: $\tau = 100$ and 150 fs for methyl ethyl and diethyl ketone, respectively (see Figs. 3 and 4). This trend would appear to be consistent with the prediction of a statistical rate theory. For example, according to the RRK theory, the rate is expressed by $k = \nu[(E - E_0)/E]^{(s-1)}$, where ν is the vibrational frequency along the reaction coordinate, E is the total available energy, E_0 is the reaction barrier, and s is the number of vibrational degrees of freedom. Therefore, since $[(E - E_0)/\mathrm{E}] < 1$, as s increases, k decreases. However, the statistical rate theory is based on the assumption that all the reactant states are equally probable through a much faster IVR rate than the dissociation. Within the dissociation time constants (50–150 fs) observed here, a complete randomization of the energy among all the reactant states is not expected.

Instead we invoke the dynamical motion of the wavepacket on the multi-dimensional potential energy surface. As the number of degrees of freedom increases with increasing number of atoms in the molecule, the wavepacket experiences motion in many coordinates other than the reaction coordinate prior to the bond dissociation and the time constant for dissociation increases. This behavior is similar to the multi-dimensional effect observed in the dissociation of CH_3I and CD_3I [27,28]. We have found a correlation between $\ln k$ and the number of modes, but in this case, the correlation reflects the probability trend in the increased phase space as the number of atoms increases.

4.3. The secondary C–C bond cleavage

After primary C–C bond cleavage, the available energy (the photon energy minus the bond dissociation energy), is partitioned into the various degrees of freedom: the translational and internal degrees of freedom of the two fragments. The secondary C–C bond dissociation occurs on the ground electronic state with a reaction barrier of ≈ 17 kcal/mol [11,25], and the dissociation dynamics are governed by the internal energy given to the intermediate during the primary α-bond cleavage. As shown in Table 1, the dissociation time constant of the CH_3CO (or C_2H_5CO) radical strongly depends on the parent molecule from which it is dissociated. This dependence means that the energy partitioning during the primary C–C bond cleavage is different for the parent molecules studied.

Here, we compare two extreme models, the impulsive and statistical models. The two models are based on completely different basic assumptions. The impulsive model assumes that all the available energy is given to the repulsion between the two carbon atoms in a very short time [17]. Therefore, the product-state distribution is determined by the impulse given to two departing atoms and the energy partitioning is determined by the conservation of energy and linear momentum [17]. On the other hand, the statistical model assumes that the energy is distributed with equal probabilities among all the states in the reactant prior to dissociation. In the statistical model, the internal energy of the fragment is determined by the ratio of the number of vibrational degrees of freedom of the fragment to that of the parent [29].

In Table 1, the time constants for the secondary C–C bond cleavage, those of the CH_3CO and C_2H_5CO radicals, are listed with the internal energies predicted from the impulsive and statistical models. According to the impulsive model, since the masses of departing atoms in the primary C–C bond cleavages are same, the internal energy given to CH_3CO is the same for acetone and methyl ethyl ketone. However, the measured time constant for the secondary C–C bond cleavage is ≈ 1.8 times larger for the CH_3CO radical produced in the dissociation from methyl ethyl ketone ($\tau_2 \approx 900$ fs) compared to that from acetone dissociation ($\tau_2 \approx 500$ fs). This experimental fact would therefore imply that the impulsive model is breaking down as more internal energy should be given to the CH_3CO radical from acetone than from methyl ethyl ketone.

On the other hand, it appears that the statistical prediction of the internal energy (Table 1) gives the correct trend. Since the C_2H_5 radical has more internal degrees of freedom than CH_3, relatively more energy is partitioned into C_2H_5, and therefore, less energy is given to the CH_3CO radical from methyl ethyl ketone, compared to that from acetone. The same explanation applies to the case of the C_2H_5CO radical from methyl ethyl and diethyl ketone: Since the departing fragment for the C_2H_5CO radical is CH_3 for methyl ethyl ketone, which takes

less energy than C_2H_5 for diethyl ketone, relatively more energy is given to the C_2H_5CO from methyl ethyl ketone, leading to a shorter time constant (550 fs) than that from diethyl ketone (750 fs).

However, this apparent trend of the statistical model does not explain the results quantitatively. This can be seen by considering several results in Table 1. The dissociation of acetyl chloride, $CH_3COCl \rightarrow CH_3CO + Cl$, is found to be prompt (< 50 fs) [7,24] and there is no internal energy to be given to the Cl atom. Therefore, the impulsive model should be appropriate in this case. The impulsive model predicts ≈ 56 kcal/mol for the CH_3CO radical from acetyl chloride. At this same energy, the CH_3CO radical from acetyl chloride has a lifetime shorter than 100 fs [24]. Given that the primary cleavage of acetone occurs in 50 fs, the impulsive model should still be appropriate; it predicts an internal energy for CH_3CO of ≈ 38 kcal/mol. However, the statistical model for acetone gives ≈ 53 kcal/mol, overestimating this value, and a much shorter dissociation time would be expected than the experimental result of $\tau_2 = 500$ fs.

The time constant for the secondary α-cleavage in acetone has been explained using the RRKM theory at the internal energy predicted by the impulsive model [15]. The internal energy of the CH_3CO radical from methyl ethyl ketone can be estimated from the measured time constant of 900 fs by using the RRKM theory [15]. The RRKM calculation is carried out using ab initio vibrational frequencies of the reactant and transition state of the acetyl radical [30]. The estimated internal energy of the CH_3CO radical from the methyl ethyl ketone photolysis is ≈ 31 kcal/mol, which is ≈ 4 kcal/mol less than the 35 kcal/mol for the acetyl radical from the acetone dissociation, Table 1.

For the internal energy of the CH_3CO radical from methyl ethyl ketone, the predicted value from the impulsive model is much different from that estimated from the RRKM calculation, especially when compared with the case of acetone. It should be noted however that the multi-dimensionality of the wavepacket in the primary α-cleavage of methyl ethyl ketone is an important factor for the decrease in the rate constant and deviation from the impulsive model. Therefore, the applicability of theoretical models for energy partitioning should be closely related to the dynamical time scale for the bond dissociation.

5. Summary and conclusion

In this work, the femtosecond dynamics of Norrish type-I reactions are reported. The dynamics of the α-bond cleavage from methyl ethyl ketone and diethyl ketone are studied using fs-resolved TOF mass spectrometry, and compared with those of dimethyl and methyl chloro ketone. In these reactions the pathways from the transition-state region are determined by two reaction coordinates along the C–C bonds, Fig. 1.

The primary and secondary α-bond cleavages occur in a *stepwise* mechanism with two distinct time scales. The time for the primary C–C bond cleavage is longer for methyl ethyl ketone and diethyl ketone, compared to that of acetone. This increase of the time constant for the primary α-cleavage with increasing number of atoms in the molecule is the result of the increased dimensionality of the potential energy surface where the wavepacket motion is significant in coordinates other than the C–C reaction coordinate. We found a correlation between the time constants and the number of degrees of freedom. The impulse in the C–C bond is caused by the σ^* repulsion.

The secondary C–C bond cleavage dynamics of the intermediates are governed by the internal energies obtained during the primary C–C bond breaking event. We considered the energy partitioning during the primary C–C bond cleavage using the impulsive, simple statistical, and RRKM models. Simple statistical calculations, although giving the correct trend, do not account quantitatively for the internal energy following the α-cleavage. The impulsive model, although not very quantitative, gives the values close to the experimental results. The transient intermediate rates of dissociation can be accounted for using RRKM theory. The key is the time scale of the cleavage in relation to IVR time scales.

In all systems studied, we find that the correct criterion for *concertedness* is the time scale for nuclear motion along the reaction coordinates. Using the criterion of the 'rotational clock', the reaction mechanism would have been inferred to be con-

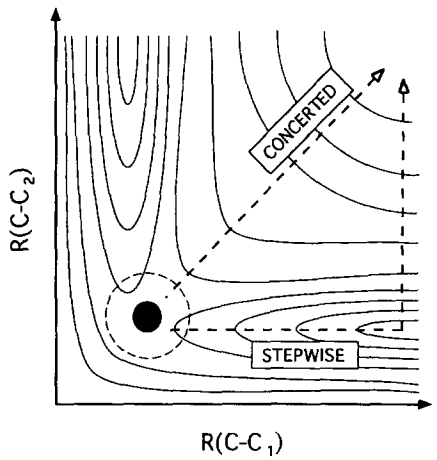

Fig. 5. A simple schematic of a two-dimensional potential energy surface illustrating the concept of concerted and stepwise motion, in principle, which describe α-cleavage reactions. The two reaction coordinates, $C-C_1$ and $C-C_2$, involved are those of R_1COR_2, where C_1 and C_2 are the carbon atoms of R_1 and R_2, respectively.

certed. In contrast, we observe that the reactions studied have stepwise mechanisms, as illustrated schematically in Fig. 5.

Acknowledgements

This research was supported by grants from the Air Force Office of Scientific Research and by the National Science Foundation. We wish to thank Mr. Ju Guo and Mr. Brent Horn for their help with some of the experiments and for useful suggestions.

References

[1] W.A. Noyes Jr., in: Photochemistry and reaction kinetics (Cambridge Univ. Press, Cambridge, 1967), and references therein.
[2] E.K.C. Lee and R.S. Lewis, Advan. Photochem. 12 (1980) 1, and references therein.
[3] N.J. Turro, Modern molecular photochemistry (Benjamin/Cummings, Menlo Park, 1978).
[4] J. Michl and V. Bonačić-Koutecký, Electronic aspects of organic photochemistry (Wiley, New York, 1990).
[5] M. Reinsch and M. Klessinger, J. Phys. Org. Chem. 3 (1990) 81.
[6] P. Brint, L. O'Toole, S. Couris and D. Jardine, J. Chem. Soc. Faraday Trans. 87 (1991) 2891.
[7] L. O'Toole, P. Brint, C. Kosmidis, G. Boulakis and P. Tsekeris, J. Chem. Soc. Faraday Trans. 87 (1991) 3343.
[8] G.C.G. Waschewsky, P.W. Kash, T.L. Myers, D.C. Kitchen and L.J. Butler, J. Chem. Soc. Faraday Trans. 90 (1994) 1581, and references therein.
[9] E.L. Woodbridge, T.R. Fletcher and S.R. Leone, J. Phys. Chem. 92 (1988) 5387.
[10] K.A. Trentelman, S.H. Kable, D.B. Moss and P.L. Houston, J. Chem. Phys. 91 (1989) 7498.
[11] G.E. Hall, D.V. Bout and T.J. Sears, J. Chem. Phys. 94 (1991) 4182.
[12] S.W. North, D.A. Blank, J.D. Gezelter, C.A. Longfellow and Y.T. Lee, J. Chem. Phys. 102 (1995) 4447.
[13] G.E. Hall, H.W. Metzler, J.T. Muckerman, J.M. Preses and R.E. Weston Jr., J. Chem. Phys. 102 (1995) 6660, and references therein.
[14] C.E. M. Strauss and P.L. Houston, J. Phys. Chem. 94 (1990) 8751.
[15] S.K. Kim, S. Pedersen and A.H. Zewail, J. Chem. Phys. 103 (1995) 477.
[16] S.A. Buzza, E.M. Snyder and A.W. Castleman Jr., submitted for publication.
[17] G. Hancock and K.R. Wilson, in: Proceedings, 4th International Symposium on Molecular Beams (Cannes, France, 1973).
[18] P.D. Lightfoot, S.P. Kirwan and M.J. Pilling, J. Phys. Chem. 92 (1988) 4938.
[19] M.J.S. Dewar, J. Am. Chem. Soc. 106 (1984) 209.
[20] W.T. Borden, R.J. Loncharich and K.N. Houk, Ann. Rev. Phys. Chem. 39 (1988) 213, and references therein.
[21] A.H. Zewail, Femtochemistry: ultrafast dynamics of the chemical bond (World Scientific, Singapore, 1994), and references therein.
[22] S. Pedersen, J.L. Herek and A.H. Zewail, Science 266 (1994) 1359.
[23] J.C. Polanyi and A.H. Zewail, Accounts Chem. Res. 28 (1995) 119.
[24] S.K. Kim, S. Pedersen and A.H. Zewail, to be published.
[25] S. North, D.A. Blank and Y.T. Lee, Chem. Phys. Letters 224 (1994) 38.
[26] P. Cossee and J.H. Schachtschneider, J. Chem. Phys. 44 (1966) 97.
[27] M.H. M. Janssen, M. Dantus, H. Guo and A.H. Zewail, Chem. Phys. Letters 214 (1993) 281.
[28] H. Guo and A.H. Zewail, Can. J. Chem. 72 (1994) 947.
[29] R.J. Campbell and E.W. Schlag, J. Am. Chem. Soc. 89 (1967) 5103.
[30] S. Deshmukh, J.D. Myers, S.S. Xantheas and W.P. Hess, J. Phys. Chem. 98 (1994) 12535.